Sub-Doppler resonances in the backscattered light from random porous media infused with Rb vapor

S. Villalba,[1] A. Laliotis,[2] L. Lenci,[1] D. Bloch,[2] A. Lezama,[1] and H. Failache[1,*]

[1]*Instituto de Física, Facultad de Ingeniería, Universidad de la República, J. Herrera y Reissig 565, 11300 Montevideo, Uruguay*

[2]*Laboratoire de Physique des Lasers UMR 7538 du CNRS, Université Paris-13, Sorbonne Paris Cité F-93430, Villetaneuse, France*

(Received 4 December 2013; published 19 February 2014)

We report on the observation of sub-Doppler resonances on the backscattered light from a random porous glass medium with rubidium vapor filling its interstices. The sub-Doppler spectral lines are the consequence of saturated absorption where the incident laser beam saturates the atomic medium and the backscattered light probes it. Some specificities of the observed spectra reflect the transient atomic evolution under confinement inside the pores. Simplicity, robustness, and potential miniaturization are appealing features of this system as a spectroscopic reference.

DOI: 10.1103/PhysRevA.89.023422 PACS number(s): 42.62.Fi, 32.30.−r, 42.25.Dd, 32.70.Jz

I. INTRODUCTION

High-quality surfaces and diffracting elements with a well controlled spatial periodicity and regularity are often considered essential properties for a proper management of light in photonics devices. Disorder and irregularity are generally avoided and minimized in the attempt to reduce the usually annoying consequences of light scattering. However, very recently a growing interest has developed for the study of disorder and irregularity in optical media and the use of diffuse light for spectroscopy purposes. Some examples are the recent advances on imaging and/or focusing through or inside highly scattering media [1–4], research on random lasers [5,6], and weak and strong Anderson localization ([7], and references therein).

The long effective path length of light in a strongly diffusing medium has been used for sensitive spectroscopic detection of molecules [8–10]. Sub-Doppler spectroscopic signals were observed in linear regime in the light reflected from an opal of nanospheres [11]. In a recent work, we have reported a study of the resonance spectroscopy of Rb inside a porous glass medium. We have shown that, as a consequence of the spatial randomization of the light wave vector due to the diffusive propagation in the porous medium, the laser photons cannot be distinguished from those spontaneously emitted by the atoms. A striking consequence is that almost no absorption is observed on the scattered light through the medium at low enough atomic vapor densities since the photons absorbed by the atoms are almost entirely compensated by fluorescence. For increased atomic density, such compensation is less effective as photon trapping increases the probability for an excited atom to collide with the pore surface and decay nonradiatively [12].

In this article we report on a study of atomic spectra observed on the light backscattered from a porous medium infused with Rb atoms. The light was collected by a photodiode at small angles (a few mrads) with respect to the incident laser beam [see Fig. 1(a)]. In spite of the smallness of the collection angles relative to the incident beam direction, these were large enough to be beyond the regime of coherent backscattering [13,14].

The main features of the spectrum consist of Doppler broadened lines corresponding to absorption by the Rb atoms present in the interstitial cavities of the porous sample near the illuminated surface [Figs. 1(b) and 1(c)]. In addition, sub-Doppler structures are also observed in the spectrum. The purpose of this article is to present the investigation of the origin and properties of these sub-Doppler features. We also address their possible use as spectroscopic references.

II. EXPERIMENTAL SETUP

The porous glass medium preparation starts with Pyrex glass grinding and rough selection of the glass grains dimensions by a mesh. A sedimentation column was used for further selection of the grain size reducing size dispersion. The glass powder was introduced in a flat-bottom Pyrex glass tube and heated to approximately 800 °C to create a rigid porous block with an excellent adhesion to the tube wall. The internal diameter of the tube is 5.5 mm. A Rb drop was distilled inside the tube under high vacuum and then the tube was sealed and separated from the vacuum setup to make what will be referred to as a porous cell. Two different porous cells were used for this work with mean pores size of 100 and 10 μm, respectively. These pore dimensions were roughly determined with an optical microscope and due to the irregularity of the interstices are mainly indicative.

The presence of Rb in the porous glass is revealed by the coloration of the sample [see Fig. 1(a)] due to the formation of Rb clusters in the glass surfaces of the interstices [15]. We observed coloration ranging from light-blue to pale-pink most probably depending on cluster size and shape. This coloration is present at every cell independently of the pore sizes considered. At normal operation the porous medium was kept at a temperature a few degrees Celsius higher than the cell Rb reservoir to avoid condensation inside the interstices. Condensation and coloration are reversible and can be easily removed by increasing the temperature of the porous medium well above the temperature of the cell Rb reservoir.

The experimental setup is shown in Fig. 1(a). A laser beam from an extended cavity diode laser is incident on the porous glass cell. The beam splitter sends part of the backscattered light to a photodiode with a detection area of 0.81 mm^2 placed 10 cm away from the porous medium

*heraclio@fing.edu.uy

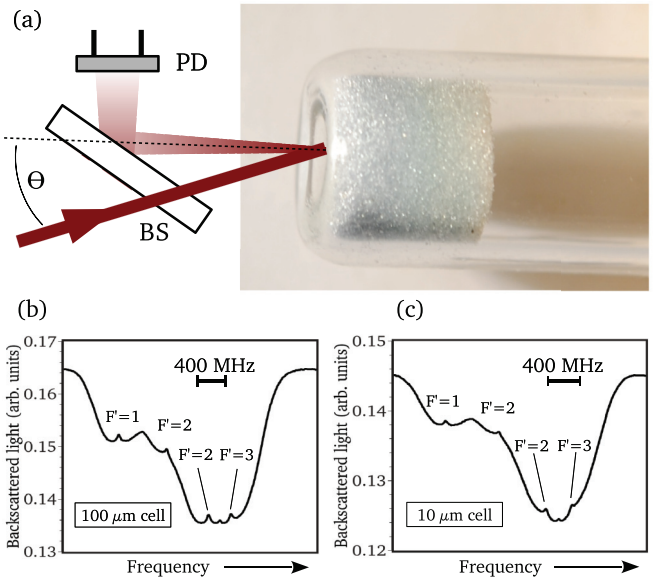

FIG. 1. (Color online) (a) Scheme of the experimental setup. Only the light scattered towards the photodetector is represented (BS: beam-splitter; PD: photodiode). (b) Backscattered light spectrum for $\theta = 0$ around the ^{85}Rb ($F = 3 \rightarrow F' = 2,3$) and ^{87}Rb ($F = 2 \rightarrow F' = 1,2$) transitions for a 100 μm porous cell, and (c) for a 10 μm porous cell.

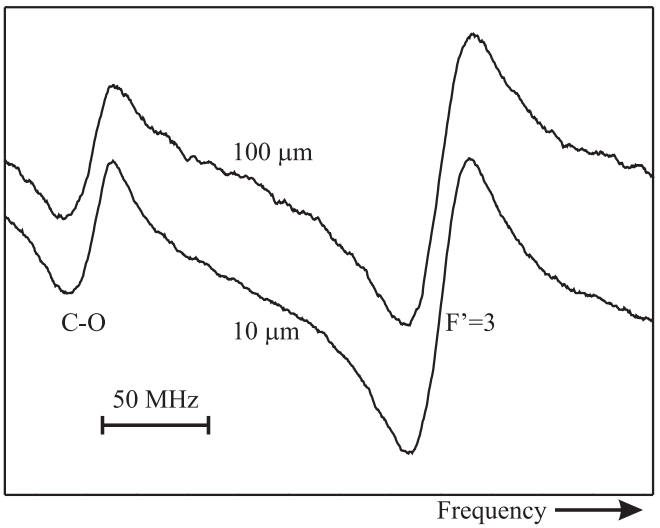

FIG. 2. Typical sub-Doppler resonances derivative recorded for the transition ^{85}Rb ($F = 3 \rightarrow F' = 3$) and nearby crossover using 6 mW light power and 2.0 mm beam diameter ($\theta = 0$). The peak-to-peak spectral widths are 29 and 32 MHz for the cells with mean pore sizes 10 and 100 μm, respectively (integration time constant 300 ms).

surface. The collection solid angle corresponds to around 10^{-5} of the detection hemisphere for the backscattered light. The porous cell was tilted with respect to the incident beam so that no reflection from the glass window at the front of the cell could reach the detector and saturate it. To increase the Rb vapor density inside the pores the cell was heated to 120 °C inside an oven (not shown). Figures 1(b) and 1(c) present spectra recorded for the cells with 100 and 10 μm pores sizes, respectively, for approximately the same experimental conditions. In these spectra the laser diode (795 nm) was tuned around the $D1$ line transitions ^{85}Rb ($F = 3 \rightarrow F' = 2,3$) and ^{87}Rb ($F = 2 \rightarrow F' = 1,2$). The Doppler broadened spectra observed in Figs. 1(b) and 1(c) correspond to a maximum reduction of 20% and 18%, respectively, of the scattered light on resonance with respect to off-resonance conditions. A noticeable feature of the spectra is the presence of sub-Doppler resonances of a few tens of MHz width.

Introducing a small modulation of the laser frequency (at around 1 kHz) and using lock-in detection we have recorded the first derivative with respect to frequency of the detected light signal (Fig. 2). The sub-Doppler spectral width was determined from these spectra by measuring the peak-to-peak frequency difference Δ_{pp}. It is worth mentioning that displacements and rotations of the porous sample relative to the incident beam do not modify in any way the observed spectra. The spectra were also not modified in a noticeable way if the reflected beam at the window of the porous cell reached the detector.

III. SUB-DOPPLER RESONANCES

It is well known that optical pumping can result in sub-Doppler spectral structures in thin cells [16] where the atomic vapor is confined between two parallel windows few to several micrometers apart. The transmission of a light beam propagating perpendicularly to the thin cell windows shows sub-Doppler structures that are the consequence of the different contribution to light absorption from the different velocity classes. Atoms with a high velocity component along the direction perpendicular to the windows have short interaction times due to the cell confinement and are not efficiently optically pumped while atoms with a low velocity component are effectively pumped. Thin cell transmission spectra are characterized by their natural width for reduced intensities and by the absence of crossover (CO) resonances. We have considered the possible occurrence of a similar mechanism in the case of atomic confinement in the interstices of the porous glass. However, the presence of CO resonances in the spectrum is not consistent with the characterization of the narrow resonances as a confinement effect. Furthermore, no sub-Doppler spectrum was observed in the light transmission through the porous medium. This is probably due to the shortness of the atomic time of flight in the interstices (a few tens to hundreds of nanoseconds) resulting in inefficient optical pumping at the low radiation intensities found inside the porous medium as a consequence of light diffusion. On the other hand, backscattered light, in which sub-Doppler spectral features are observed, mostly originates near the sample surface where the radiation intensity is higher. This suggests that the observed sub-Doppler resonances are mainly due to a saturated absorption mechanism.

Saturated absorption (SA) spectroscopy requires a pump beam and a counterpropagating probe beam that interact nonlinearly with the atoms. Although inside the bulk of a diffusive medium light beams are not well defined, one can consider that near the light entrance surface of the porous sample the pump beam corresponds to the incident laser

radiation that propagates into the porous medium a distance of the order of the scattering mean free path length without significant change in the wave vector direction. Depending on the porosity of the medium, the mean free path distance ranges from a few microns to several tens of microns [17]. Such radiation propagating forward near the sample surface produces a velocity-selective saturation in the atomic vapor which is probed by radiation scattered backwards in the direction determined by the position of the detector. Narrow Lamb dips are expected in the backscattered light at the atomic resonance frequencies as well as CO dips at the middle frequency between any two atomic resonances [18].

IV. SUB-DOPPLER RESONANCES BROADENING MECHANISMS

A. Residual Doppler broadening

We have examined the dependence of the width of the SA resonances with the detection angle θ between the incident beam and the center of the detector seen from the illuminated spot on the sample surface [see Fig. 1(a)]. The detection angle was modified by simply changing the detector position.

Figure 3 shows the experimentally observed variation of the SA resonance width Δ_{pp} as a function of θ for two porous samples and for a standard spectroscopic Rb cell at room temperature (notice that for a Lorentzian profile Δ_{pp} is smaller than the FWHM width by a factor $\sqrt{3}$). A residual Doppler broadening is present in all cases with an approximately linear dependence on θ except at small angles where other broadening mechanisms are dominant. The minimum value for Δ_{pp} in the standard spectroscopic cell appears to be larger than the natural width ($5.8/\sqrt{3}$ MHz) most probably due to

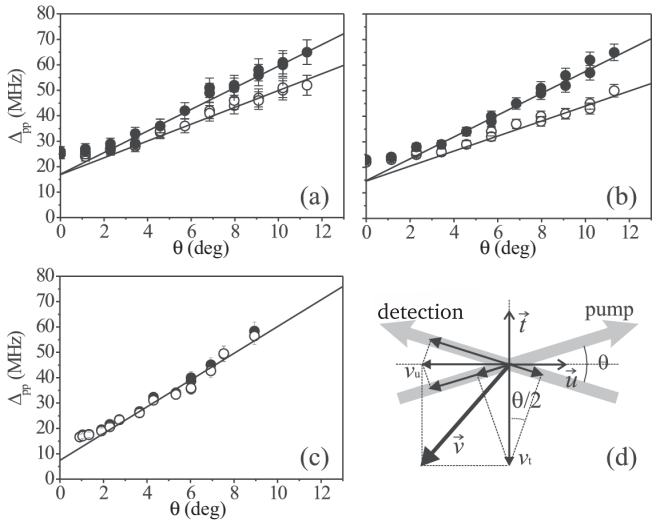

FIG. 3. Doppler broadening as a function of the detection angle θ for the 100 μm cell (a) and for a 10 μm cell (b) using a 5 mW and 2 mm diameter incident beam. (c) Doppler broadening as a function of the angle θ between the probe (10 μW, 3.0 mm diameter) and pump beam (500 μW, 3.0 mm diameter) in a standard cell (full circles: single transition resonance; open circles: CO resonance; continuous line: linear fit for large angles). (d) Beam configuration considered for saturated absorption spectroscopy.

power broadening and to a significant laser width (~4 MHz), with only a small contribution of Rb-Rb collisions [19]. An additional broadening mechanism plays a role in the porous media as will be discussed below.

Figures 3(a) and 3(b) show the measured variation of the sub-Doppler resonances width Δ_{pp} as a function of the scattered light detection angle θ for the cell with mean pore sizes of 100 and 10 μm, respectively. It is interesting to notice that unlike the standard cell where the single transition resonances and CO essentially have the same width [Fig. 3(c)], in the porous medium the CO are systematically narrower for a given angle than the single transition resonances. Moreover, the width of the CO relative to the single transition resonance is smaller in the sample with smaller mean pore size. Also, for a given angle, the linewidths are narrower in the porous cells compared to the standard cell.

In order to discuss the significance of these results let us consider the SA configuration shown in Fig. 3(d). It is useful to decompose the atomic velocity along the unit vectors $\vec{u}$ and $\vec{t}$ oriented along the bisectors of the angles between pump and probe beams. For an atom of velocity $\vec{v}$ to be simultaneously resonant with the two fields, the velocity component $v_u \equiv \vec{v} \cdot \vec{u}$ must satisfy $v_u = 0$ for the single resonance peaks and $k\cos(\theta/2)v_u = (\omega_1 - \omega_2)/2$ in the case of the CO between transitions at frequencies ω_1 and ω_2. The transverse velocity $v_t \equiv \vec{v} \cdot \vec{t}$ is determined by the laser frequency through $k\sin(\theta/2)v_t = \delta$ where δ is the laser detuning in the laboratory reference frame relative to the transition frequency in the case of a single resonance peak or relative to the mean frequency $(\omega_1 + \omega_2)/2$ in the case of the CO [18].

For a given laser detuning the number of atoms simultaneously interacting with the two laser fields is $N(\delta) \propto \mathcal{N}(v_u, \frac{\delta}{k\sin(\theta/2)})$, where $\mathcal{N}(v_u, v_t)$ is the atomic velocity distribution in the $\vec{u}, \vec{t}$ plane.

When the angle between the pump and the probe fields is large enough for the residual Doppler broadening to be much larger than the homogeneous linewidth, the shape of the SA resonance is mainly determined by the number of atoms that have been resonantly excited by the two fields *and* efficiently optically pumped. For sufficiently large angles, if the interaction time between the atoms and the light is assumed to be long enough to allow efficient optical pumping independently of the atomic velocity, then the SA signal line shape is proportional to $N(\delta)$. In the standard spectroscopic cell one can assume that $\mathcal{N}(v_u, v_t)$ follows the Maxwell-Boltzmann distribution in which case the dependence on the two velocity components factorize and $N(\delta)$ is a Gaussian of width Δ_{Dopp}. Consequently the width of the SA transitions for large enough θ should be given by $\Delta_{\mathrm{Dopp}}\sin(\theta/2)$.

In the porous medium the atom confinement introduces an effective limitation on the atomic velocity in order for an atom to interact with the light *and* be efficiently optically pumped. The typical magnitude of the limiting velocity v_L can be estimated as $v_L = L/T$ where L is the mean free pass of the atoms in the pores and T a characteristic optical pumping time. The existence of v_L introduces a constraint in the distribution of atoms effectively interacting with the light as a function of the two orthogonal velocity components since

$v_u^2 + v_t^2 < v_L^2$ must hold. In the case of the single transition resonances where $v_u = 0$, the transverse velocity v_t of the atoms participating in the process is bounded by v_L, while in the case of the CO where $v_u \neq 0$, the transverse velocity is bounded to a maximum value smaller than v_L. Based on these simple qualitative considerations one can expect a narrower effective transverse distribution and consequently a narrower residual Doppler width, for the porous media than for the standard cell (where $v_L \sim \infty$ is generally assumed). The same argument justifies the fact that narrower residual Doppler widths are observed for the CO than for the single transition lines in the porous sample. From this perspective, the observed differences in residual Doppler linewidth between the standard cell and the porous media, and between the the CO and the single transition resonances appear to be a direct manifestation of atomic confinement.

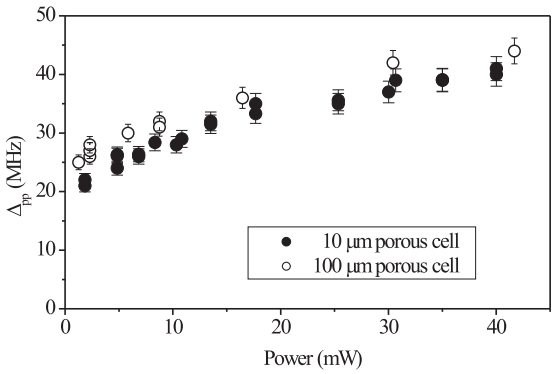

FIG. 4. Power broadening measured for a single transition resonance on the two porous cells as a function of the incident beam power ($\theta \cong 0$, beam diameter: 2 mm).

B. Light fields wave-vector spreading

We now discuss the SA resonances width observed under a small detection angle $\theta \sim 0$. The finite detection *solid* angle of the probe radiation constituted of diffuse light, and the finite size of the illuminated area of the sample (typically a 2 mm diameter circle) determines the spreading of the probe field wave vector which results in broadening of the SA resonances. At low intensities this broadening mechanism was revealed as the dominant contribution to the linewidth. The influence of the detection solid angle on the broadening of the SA resonances was confirmed experimentally by varying the solid angle with the use of a lens.

C. Transit time

In addition to atomic collisions and saturation effects that are present in standard spectroscopic cells, atomic confinement introduces an additional broadening mechanism since it limits an effective atom-light interaction time. Transit time effects in SA were studied both theoretically [20,21] and experimentally [22–25]. A crude estimation of the transit time τ would be $\bar{v}/L$, where $\bar{v}$ is the mean atomic velocity. This would result in a linewidth of the order of τ^{-1} [18]. However, this is certainly an overestimation since due to the nonlinearity of SA, the contribution of slow atoms or atoms with long interaction times is expected to be relatively more important than the contribution of fast atoms or atoms with short interaction times, resulting in narrowing of the SA spectrum [20]. Transit time broadening plays an important role in SA of Rb in hollow-core fibers [26].

The minimum SA width measured in the 10 μm porous medium (Figs. 3 and 4) would correspond to a transit time broadening of 25 MHz. However, if transit time is the dominant broadening mechanism, narrower spectral lines are expected for the 100 μm cell. Instead, broader spectra were systematically observed for this cell indicating that also other broadening mechanisms must be considered.

One possible mechanism arises from taking into account the atomic resonant fluorescence. Photons emitted by the atoms, which are indistinguishable from the laser photons, effectively result in additional spreading of the pump and probe fields wave vectors. Since collisions with the pore walls quenches the fluorescence [12], the relative contribution of fluorescence-induced broadening is expected to be larger in the 100 μm cell than in the 10 μm where significant fluorescence quenching is expected.

D. Power broadening

Most of the measurements on porous cells were done using a saturating incident beam. Although the intensity of the light interacting with the atoms was expected to be largely reduced after propagation in the porous medium as a consequence of light diffusion, the atoms contributing to the observed SA spectra were supposed to be close to the surface of the porous medium irradiated by the incident beam. In order to experimentally account for the power broadening of the SA spectra we measured its spectral width Δ_{pp} for different intensities of the incident beam. As can be seen in Fig. 4 the power broadening mechanism makes an important contribution to the spectral width. Nevertheless the minimum width extrapolated at zero intensity still has a significantly large value compared to the natural width.

Although transit time broadening should not be negligible for the cell with smaller pores, we consider that the SA spectral width for $\theta = 0$ and at low intensities is mostly dominated by the intrinsic broadening mechanism related to the laser fields wave-vector spreading that is additionally increased by the atomic fluorescence.

V. SUB-DOPPLER RESONANCES CONTRAST

Confinement effects are also present when comparing the SA line contrast. The contrast of the SA spectra, defined as the ratio of a SA resonance amplitude to the amplitude of the Doppler broadened background, is a function of the light intensity. The contrast measured for the transition ^{85}Rb ($F = 3 \rightarrow F' = 2$) in the spectra shown in Figs. 1(b) (100 μm cell) and 1(c) (10 μm cell) are, respectively, 5.1% and 4.5%. The highest observed contrast was around 7%. Higher contrast was systematically measured for the 100 μm in comparison to the 10 μm cell for the same light intensity. This is in agreement with the expectation of a more efficient optical pumping in the cell with larger pores.

We also observed that the CO between the transitions ^{85}Rb ($F = 3 \rightarrow F' = 2,3$) has an amplitude [relative to the ^{85}Rb ($F = 3 \rightarrow F' = 2$) resonance] larger by approximately 15% in the 100 μm pores cell than in the 10 μm pores cell. For both cells the CO amplitude (relative to the single transition lines amplitude) increases with light intensity. These results are consistent with the fact that the atoms contributing to the CO correspond to large velocities and thus have small interaction times due to the pore confinement.

Due to the random nature of the polarization of the light scattered by the sample, we did not observe significant variation of the SA resonances contrast by using polarization selective detection.

VI. CONCLUSIONS

The experimental setup presented here for sub-Doppler spectroscopy is extremely simple and robust. It bears the remarkable property of being completely independent of the orientation of the porous medium and insensible to its displacements. The spectra are only slightly dependent on the angle of the detector with respect to the backscattering direction. The signal amplitude can then be increased by an enlargement of the detection solid angle without a significative penalization on the spectral width. Spectra recorded at the 10 μm cell using a beam diameter of 200 μm and only 130 μW of optical power have a typical signal-to-noise ratio of $\sim$50. This result suggests that a porous glass block of a few hundred microns can be used as a miniaturized spectroscopic cell [27,28]. One possible way to implement such cell would be to cut a Rb-filled large porous sample into smaller pieces while at the same time sealing the external surface through glass melting. We are currently exploring this possibility.

ACKNOWLEDGMENTS

The authors acknowledge the support of ANII, CSIC, and PEDECIBA Uruguayan agencies, and ECOS-Sud, CREI, and ANR 08-BLAN-0031 French projects.

[1] E. G. van Putten, D. Akbulut, J. Bertolotti, W. L. Vos, A. Lagendijk, and A. P. Mosk, Phys. Rev. Lett. **106**, 193905 (2011).
[2] O. Katz, E. Small, Y. Bromberg, and Y. Silberberg, Nat. Photonics **5**, 372 (2011).
[3] I. M. Vellekoop, A. Lagendijk, and A. P. Mosk, Nat. Photonics **4**, 320 (2010).
[4] B. Judkewitz, Y. M. Wang, R. Horstmeyer, A. Mathy, and C. Yang, Nat. Photonics **7**, 300 (2013).
[5] D. S. Wiersma, M. P. van Albada, and A. Lagendijk, Phys. Rev. Lett. **75**, 1739 (1995).
[6] Q. Baudouin, N. Mercadier, V. Guarrera, W. Guerin, and R. Kaiser, Nat. Phys. **9**, 357 (2013).
[7] M. Segev, Y. Silberberg, and D. N. Christodoulides, Nat. Photonics **7**, 197 (2013).
[8] T. Svensson, M. Andersson, L. Rippe, J. Johansson, S. Folstad, and S. Andersson-Engels, Opt. Lett. **33**, 80 (2008).
[9] T. Svensson and Z. Shen, Appl. Phys. Lett. **96**, 021107 (2010).
[10] T. Svensson, E. Adolfsson, M. Lewander, C. T. Xu, and S. Svanberg, Phys. Rev. Lett. **107**, 143901 (2011).
[11] P. Ballin, E. Moufarej, I. Maurin, A. Laliotis, and D. Bloch, Appl. Phys. Lett. **102**, 231115 (2013).
[12] S. Villalba, H. Failache, A. Laliotis, L. Lenci, S. Barreiro, and A. Lezama, Opt. Lett. **38**, 193 (2013).
[13] M. P. Van Albada and A. Lagendijk, Phys. Rev. Lett. **55**, 2692 (1985).
[14] P.-E. Wolf and G. Maret, Phys. Rev. Lett. **55**, 2696 (1985).
[15] A. Burchianti, A. Bogi, C. Marinelli, C. Maibohm, E. Mariotti, and L. Moi, Phys. Rev. Lett. **97**, 157404 (2006).
[16] S. Briaudeau, D. Bloch, and M. Ducloy, Phys. Rev. A **59**, 3723 (1999).
[17] In addition to the effect of the glass porosity, the bottom of the glass tube has some curvature resulting in lensing effect producing additional spreading of the light propagation direction. We have neglected the lensing effect in our discussion.
[18] W. Demtroder, *Laser Spectroscopy* (Springer-Verlag, Berlin, 1996).
[19] K. Niemax, M. Movre, and G. Pichler, J. Phys. B **12**, 3503 (1979).
[20] C. Bordé, J. Hall, C. Kunasz, and D. Hummer, Phys. Rev. A **14**, 236 (1976).
[21] E. Baklanov and B. Y. Dubetskii, Sov. J. Quantum Electron. **18**, 857 (1988).
[22] S. Bagaev, A. Baklanov, A. Dychkov, P. Pokasov, and V. Chebotaev, JETP Lett. **45**, 471 (1987).
[23] S. Bagayev, A. Baklanov, V. Chebotayev, and A. Dychkov, Appl. Phys. B **48**, 31 (1989).
[24] C. Chardonnet, F. Guernet, G. Charton, and C. Bordé, Appl. Phys. B **59**, 333 (1994).
[25] J. Hald, J. C. Petersen, and J. Henningsen, Phys. Rev. Lett. **98**, 213902 (2007).
[26] A. D. Slepkov, A. R. Bhagwat, V. Venkataraman, P. Londero, and A. L. Gaeta, Phys. Rev. A **81**, 053825 (2010).
[27] W. Yang, D. B. Conkey, B. Wu, D. Yin, A. R. Hawkins, and H. Schmidt, Nat. Photonics **1**, 331 (2007).
[28] S. A. Knappe, H. G. Robinson, and L. Hollberg, Opt. Express **15**, 6293 (2007).